EFFECT OF TEMPERATURE ON CALCIUM CARBONATE DEPOSITION IN SITU ON BAMBOO FIBER AND POLYMER INTERFACES

Haitao Cheng
Assistant Professor
College of Materials Science and Technology
Beijing Forestry University
Beijing, China 100083
International Center for Bamboo and Rattan
Beijing, China 100102
E-mail: htcheng@icbr.ac.cn

Jie Gao
Graduate Research Assistant
E-mail: gaojie2009@icbr.ac.cn

*Ge Wang**†*
Professor
International Center for Bamboo and Rattan
Beijing, China 100102
E-mail: wangge@icbr.ac.cn

Sheldon Q. Shi†
Associate Professor
Department of Mechanical and Energy Engineering
University of North Texas
Denton, TX
E-mail: Sheldon.Shi@unt.edu

*Shuangbao Zhang**
Professor
College of Materials Science and Technology
Beijing Forestry University
Beijing, China, 100083
E-mail: shuangbaozhang@163.com

Liping Cai†
Research Associate
Department of Mechanical and Energy Engineering
University of North Texas
Denton, TX
E-mail: liping.cai@unt.edu

(Received August 2013)

* Corresponding author
† SWST member

Wood and Fiber Science, 46(2), 2014, pp. 247-258

Abstract. The objective of this work was to investigate the effect of different reaction temperatures on the mechanical and surface (interface) properties of calcium-carbonate ($CaCO_3$)-filled bamboo fibers and polypropylene (PP) composites. With an ionic reaction of sodium carbonate and calcium chloride aqueous solution at various bath temperatures, $CaCO_3$ particles were successfully deposited in situ on bamboo fibers. Polymer composites were fabricated using treated bamboo fibers as the reinforcement and PP as the matrix. Tensile tests of single fibers and PP composites were performed to determine the mechanical properties at different conditions. Results showed that the treatments improved compatibility between bamboo fibers and PP matrix, and the crystallinity of inorganic materials was affected by the treatment temperature. Compared with the composites reinforced with untreated bamboo fibers, the tensile strength and modulus of composites reinforced with treated fibers increased by 14.58 and 19.66%, respectively.

Keywords: Calcium carbonate, bamboo fibers, interface/interphase, poly(propylene) (PP), composites, mechanical properties.

INTRODUCTION

Recently, biobased wood–polymer composites (WPC) have been receiving considerable attention because of their low processing cost, biodegradation, and improved physical, mechanical, and biological performance. The global WPC industry is worth at least $2 billion in the decking, railing, automotive, and consumer market (Jacob 2006). Compatibility between the fiber surface and polymer matrix has been a major issue for cellulosic fiber-reinforced polymer composite processing. Coupling agents are widely used to modify the interface between hydrophilic cellulose fibers and hydrophobic polymers to improve mechanical properties of composites (Raj et al 1990). However, the organic coupling agents are usually costly and also raise environmental concern.

Manufacturing defects in composites, such as interfacial failure and air pockets, could be caused by numerous micropores in the cell wall structure of cellulosic fibers. Hence, it was reported that the interface compatibility could be improved because nanoparticles impregnated on the fiber surface with high temperature and pressure conditions served as nucleation sites (Allan et al 1992; Alexandre and Dubois 2000; Biswas and Ray 2001; Schmidt et al 2002; Shi et al 2011; Chen and Yan 2012, 2013). The depositing process in situ was also applied in pulp to improve internal bonding and tensile strength of paper (Lutton 1952; Green 1985; Kuusipalo et al 2005). Incorporation of fillers such as mica, kaolin, calcium carbonate ($CaCO_3$), and talc into polymer composites is common practice in the plastics industry and can decrease the production costs of molded products. Fillers can also improve other properties, such as strength, rigidity, durability, and hardness (Khunová et al 1999). The increase in the strength of the composites from incorporating fillers is attributed to the homogeneously dispersed particles because the well-dispersed particles made the crack propagation path longer, absorbed a portion of the energy, and enhanced plastic deformation (Leong et al 2004). Various dispersing agents, such as $CaCO_3$, talc, and mica, for the inorganic particles have been investigated (Altay et al 2007; Deka and Maji 2011). It might be difficult to impregnate the nanoparticles into the micropore cell wall structure of the cellulosic fibers with a high temperature and pressure process. In the $CaCO_3$ particles impregnation process in this study, the primary salt $CaCl_2$, secondary ionic salt Na_2CO_3, and complexing agent ethylenediamine tetraacetic acid (EDTA)-2Na (Gopi and Subramanian 2012) were impregnated stepwise.

It was expected that the impregnation of the inorganic nanoparticles into the micropore structure of the fiber cell walls would decrease the microvoid volume in fibers and decrease air bubble formation during the composite fabrication process. As a result, a simple (the inorganic nanoparticles were formed directly) process with low cost (using inexpensive ionic salts) and minor environmental concern (reusing weak chemical solutions) would be obtained. The products can be potentially used as vehicle components

because of their light weight, good mechanical properties, and environmental friendliness.

Heating temperature had a significant effect on crystallinity of $CaCO_3$ with EDTA-2Na (Gopi and Subramanian 2012). In this study, bamboo fibers were deposited with $CaCO_3$ in situ at different treatment temperatures. The objective of this study was to optimize the treatment temperature for bamboo fibers by evaluating property improvement of bamboo fiber–polypropylene (PP) composites.

MATERIALS AND METHODS

Materials

Bamboo culms were obtained from 3-yr-old Cizhu bamboo (*Neosinocalamus affinis*) grown in Changning County, Sichuan Province, China. Specimens of 20 mm (longitudinal) × 2 mm (radial) × 2 mm (tangential) were cut from the middle section of bamboo (about 1.5-3.0 m from the ground) and air-dried to about 12% MC.

All chemicals were of analytical grade and were provided by Sinopharm Chemical Reagent Beijing Co., Ltd. (Beijing, China). Sodium carbonate (Na_2CO_3) and calcium chloride ($CaCl_2$) were digested into 0.1 mol/L aqueous solution with distilled water. Disodium salt of EDTA-2Na was applied as crystalline control agent, and hydrogen peroxide (H_2O_2) and glacial acetic acid (HAc) were used as impregnating agents.

PP films (CoEx oriented PP) with a density of 905 kg/m^3 and a thickness of 0.5 mm were provided by Beijing Jixing Trading Co. (Beijing, China).

Fiber Preparation

Air-dried bamboo strips were immersed in a solution of H_2O_2 and HAc (at a molar ratio of 1:1) and kept at 60°C for 24 h to separate the fibers (Chen et al 2011a, 2011b; Wang et al 2011). All obtained fibers were taken out and washed thoroughly with tap water and then with deionized water five times. After separating mechanically using fine tweezers, individual fibers (tracheids) were air-dried to equilibrium moisture content in ambient conditions.

A flowchart on the treatment details is presented in Fig 1. At temperatures of 5, 15, 25, 45, or 65°C, the air-dried bamboo fibers and 0.1 mol/L $CaCl_2$ aqueous solution (1:50 g/mL) were placed in a round bottom flask and stirred for 20 min. During the vigorous magnetic stirring, equal volumes of the chemical additive (1.7 g/L) and Na_2CO_3 (0.1 mol/L) aqueous solution were added drop by drop. The resulting mixture was aged for 25 min at the same temperature. Excess $CaCO_3$ particles between fibers and other byproducts were removed by running water. For comparison, single fibers were also obtained by magnetic stirring at 25°C for 20 and 25 min using the same chemical additive. Afterward, the retted fibers as control samples and the treated fibers were placed in a conditioning chamber with a preset temperature of 20°C and RH of 65%.

Single Fiber Characterization

Surface morphology analysis. An FEG-XL30 environmental scanning electron microscope (ESEM) with an accelerating voltage of 10 kV was used for examining the morphology of the

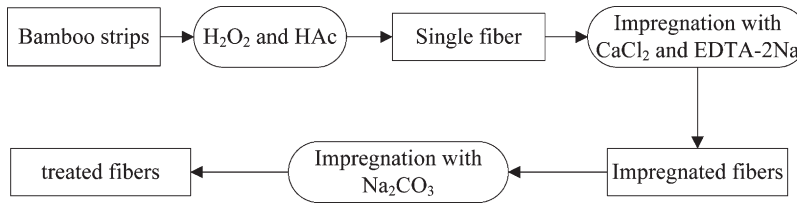

Figure 1. Flowchart of treated bamboo fibers.

treated fibers. Prior to analysis, the fracture surfaces were coated with a layer of gold using a sputtercoater. Eighty fibers from each digestion temperature were randomly selected, and images were taken with ESEM. Dimensions of the particles of $CaCO_3$ deposited on the bamboo fiber surface were measured by image analysis. Elemental analysis of mineral-containing composites was also performed with ESEM coupled with an energy dispersive X-ray spectrometer (EDS). Two hundred fibers from each treatment were randomly selected, and dimensions of the fibers were measured by image analysis. The distributions of their length, diameter, and aspect ratio were statistically examined.

Surface roughness analysis. Roughness of the individual fiber coated with $CaCO_3$ was analyzed using an atomic force microscopy (AFM), Bruker Instruments (Billerica, MA), model ICON. Micrographs were obtained in tapping mode under ambient conditions using the Tap300 tips. Fiber surfaces were imaged with a 5 × 5-μm scan size with a scanning frequency of 0.5 Hz. Roughness data were measured using NanoScope analysis software (version 1.40). The principle of fractal dimension estimation from AFM images was reported previously by Mannelquist et al (1998) and Tang and Wang (2012).

Contact angle measurement. Contact angle (CA) determination of distilled water droplets on individual fibers was performed by the sessile drop technique in a video-based system DSA100 with a humidity control unit (Hamburg, Germany) at 22 ± 1°C and 50 ± 10% RH (Chen et al 2011a, 2011b; Cheng et al 2013). A sessile drop of 10 μL was gently put on the surface of the single fibers by means of a continuous nanoliter injection mode with microquartz dosing. Initially, digital images of the drop were taken at a rate 72 frames/s in DSA 3 software by a CCD camera. The method used to fit a mathematical function (Yamaki and Katayama 1975) to the measured drop contour line was the ellipse method. In this method, a line of an ellipse approximates the drop contour and deviations from the true drop shape are minimal (Yamaki and Katayama 1975; Amaral et al 2002). The ellipse method leads to satisfying precision in the CA and has been applied by a number of researchers (Wu and Dzenis 2006). For each treatment combination, more than 15 samples were evaluated.

Determination of $CaCO_3$ loading. The percentage of $CaCO_3$ loaded in the fibers was calculated based on the difference in ash contents between the untreated and treated fibers. The ash content was determined by burning the material in a muffle furnace (Carbolite CMF 1300; Carbolite Limited, Hope Valley, UK) at 575°C for 4 h in accordance with GB (2009). Two duplicates were completed for each level with a maximum error of 0.2%.

Tensile properties. Single-fiber tension tests were conducted using an Instron (Norwood, MA) 5848 universal material-testing machine with an SF microtester module designed at the International Center of Bamboo and Rattan (Beijing, China) (Fig 2). With assistance from a stereomicroscope, fibers were first placed across a slot of 1.8 mm in a Plexiglas plate and then two ends of the fiber were taped to the rims of the slot (Wang et al 2011). The fibers were then placed in an oven at 60°C for 24 h. Individual fibers were measured in a humidity chamber with 23 ± 2°C, 40 ± 5% RH, and a constant tensile rate of 0.048 mm/min. Fibers were removed from the tensile clamps immediately upon failure, and subsequently, the cross-sectional area was measured with a confocal laser scanning microscope (CLSM, Zeiss LSM 510 Meta; Carl Zeiss Microscopy, Jena, Germany) for tensile modulus and stress calculations. The values of elongation at the break, tensile modulus, and stress were averages of 30 samples for each individual bamboo fiber. A multiple comparison with Fisher's least significant difference method at $\alpha = 0.05$ was carried out with SPSS software.

Composite Fabricating

The composites were fabricated with a compression molding process. The control and treated bamboo fibers were dispersed in water by vigorous mechanical stirring. The fiber suspension

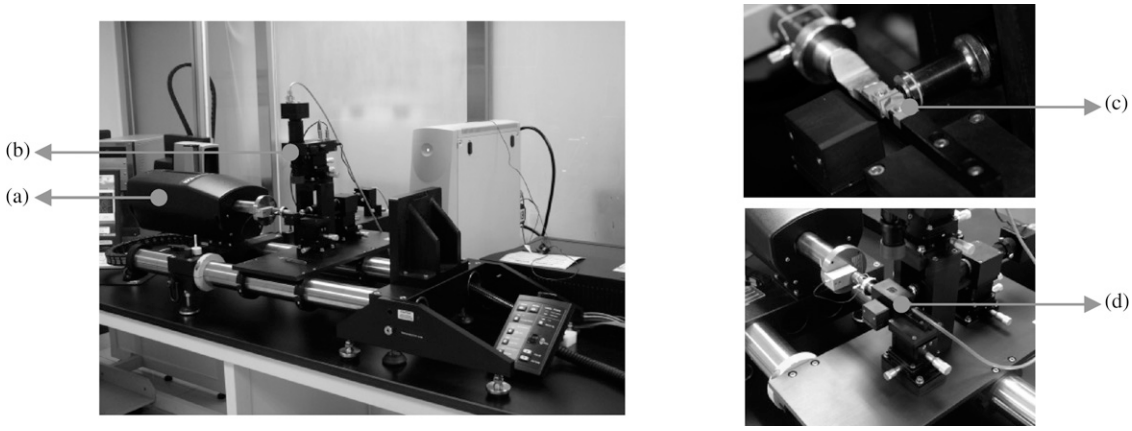

Figure 2. Single-fiber tensile testing instrument. (a) Instron 5848 universal material-testing machine; (b) SF-microtester module designed at the International Center of Bamboo and Rattan; (c) clamp; (d) humidity chamber.

was poured into a sand core funnel and then formed into fiber sheets using a vacuum filtration method. The fiber sheets were dried to 2% MC at 103°C and were placed in a desiccator with the anhydrous $CaCl_2$.

The fiber sheets and PP films were cut to 150 × 150 mm and laminated alternately. The weight ratio of fiber to PP in the composite panel was 1:2. The laminated mats were pressed at 180°C and 2.0 MPa for 2.0 min. The pressure was not released until the platen cooled to room temperature. Before the property tests, the bamboo fiber–PP panels were removed from the press and placed in an oven with air circulating at 25°C and 50% RH for 48 h. Three panels with a thickness of 0.5 mm were fabricated.

Tensile Properties of Composites

After conditioning in an air-circulating oven, tensile property of the treated fiber–PP composites and untreated fiber–PP composites were measured with an Instron Universal material-testing machine 5848 (load cell 500 N) in accordance with standard GB1040.3-2006-T with type 5 testing (GB 2006). The crosshead extensions were used as specimen deformations. The crosshead rate during the tension tests was 2.0 mm/min, and each tensile value was the average of at least five specimens. All tests were carried out in an air-conditioned room at 25°C. Multiple comparison of the results was conducted with Fisher's least square method at $\alpha = 0.05$ using SPSS software. The fracture surfaces of the samples were observed using ESEM.

RESULTS AND DISCUSSION

Elemental Analysis

To investigate the dispersion of $CaCO_3$ on individual bamboo fibers, the EDS spectrum and the EDS elemental mapping were tested (Figs 3 and 4). The fibers were coated by $CaCO_3$ particles, which were formed with 0.1 mol/L $CaCl_2$ and $NaCO_3$ solution at 25°C. The EDS spectrum shows that the sample consisted of calcium (Ca), carbon (C), and oxygen (O) indicating that the

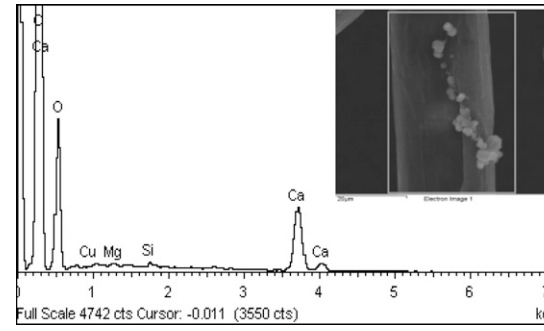

Figure 3. Energy dispersive X-ray spectrometer spectrum of treated bamboo fiber. The rectangle designates the point that was analyzed.

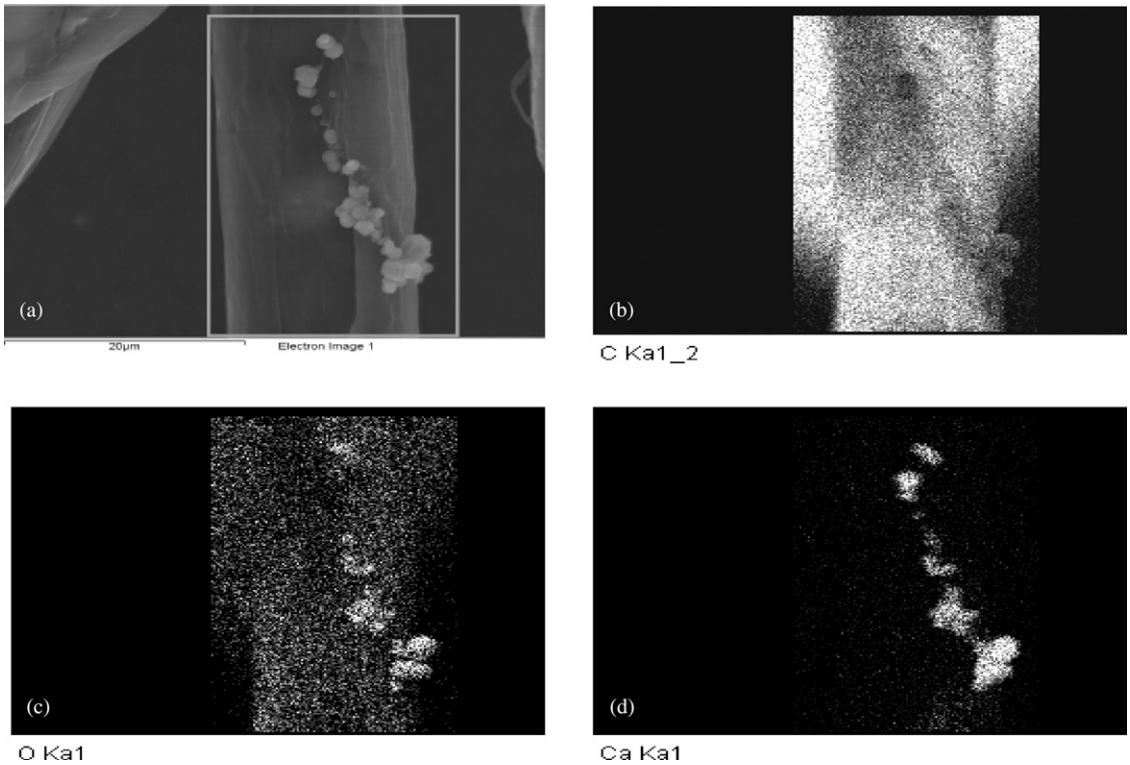

Figure 4. Energy dispersive X-ray spectrometer elements mapping of treated bamboo fibers. (a) scanning electron microscope image; (b) carbon (C); (c) oxygen (O); (d) calcium (Ca).

$CaCO_3$ nanoparticles existed in the fibers. Calcium can only exist in $CaCO_3$ because neither sodium (Na) nor chlorine (Cl) was detected from the EDX. Therefore, this evidence shows that the reaction between Na_2CO_3 and $CaCl_2$ occurred during the treatment process and the $CaCO_3$ was synthesized. Figure 4b-d shows the EDS elemental mapping images of C, O, and Ca, respectively, from which it can be seen that the Ca element was well distributed.

Effect of $CaCO_3$ Loading

The loading percentage of $CaCO_3$ in the fibers is shown in Table 1. Each specimen was examined twice with a maximum error of 0.2%. Table 1 illustrates that the fibers treated at 25°C had the highest $CaCO_3$ loading and $CaCO_3$ particle sizes were mainly distributed between 30 nm and 1 mm. As temperature increased, the inorganic nanoparticle size increased, indicating that temperature played an important role in the formation of $CaCO_3$ crystals. A small increase in $CaCO_3$ nanoparticle loading could result in a significant change in surface characteristics of the fibers because the impregnated particles were in nano or micron scales with a high specific surface area (Shi et al 2011). Therefore, a small amount of $CaCO_3$ nanoparticles would present a large surface area, which may have a significant impact on the interfacial compatibility between the fiber and the polymer matrix.

Table 1. $CaCO_3$ loading percentages and range of particle sizes on treated bamboo fibers.

Treated conditions (°C)	$CaCO_3$ loading (%)	Range of particle sizes (mm)
5	1.01	30-50
15	1.57	30-430
25	2.34	30-683
45	1.49	30-789
65	1.61	30-997

Surface Morphology

Without mechanical damages, these fibers had consistent distribution in length, diameter, and aspect ratio, because they performed the sole ionic reaction of Na_2CO_3 and $CaCl_2$ aqueous solution. The length, diameter, and aspect ratio of the fibers ranged from 0.91-3.07 mm, 0.015-0.029 mm, and 44.83-142.65 mm, respectively.

Surface morphology of treated bamboo fibers is shown in Fig 5. Figure 5a presents the untreated fiber surfaces with visible micropores, such as pits and longitudinal wrinkles formed during air-drying. These micropores could be generated because of the removal of hemicelluloses and lignin (Wan et al 2010), which would benefit the impregnation of ionic solutions along the fibers and provide sites for $CaCO_3$ crystal deposition (Allan et al 1992). Because the nucleation rates of $CaCO_3$ crystals decreased at low temperatures, a few nanoparticles occurred in the pores of bamboo fibers at 5°C. The crystals appeared single and irregularly tetrahedral with hierarchical structures (Huang et al 2007). As shown in Fig 5d-f, as the temperature ascended, $CaCO_3$ particle size became larger, and more pits and wrinkles were filled. The polymorph changed from irregular tetrahedron to spherical or ellipsoidal, and the range of particle size was enlarged. Only a binary mixture of rhomboidal calcite and vaterite occurred with EDTA (di sodium salt) at 60°C (Gopi and Subramanian 2012). As the $CaCO_3$ particles continued to grow, the micropores could not be filled any more. The bigger particles adsorbed on the surface would be formed and removed during washing with running water. As a result, $CaCO_3$ declined slightly as the temperature rose in the latter process.

Surface Roughness

The surface roughness characteristics of the samples were evaluated using intermittent tapping mode AFM by Rq defined as the standard deviation of the height values within the scanned area (Table 2). The results showed that the mean values for Rq of treated bamboo fibers coating $CaCO_3$ particles were significantly lower than that of the control. It became obvious that the average value of Rq decreased and then increased with an increase in temperature and reached a minimum value at 25°C. However, the improvement in surface roughness was

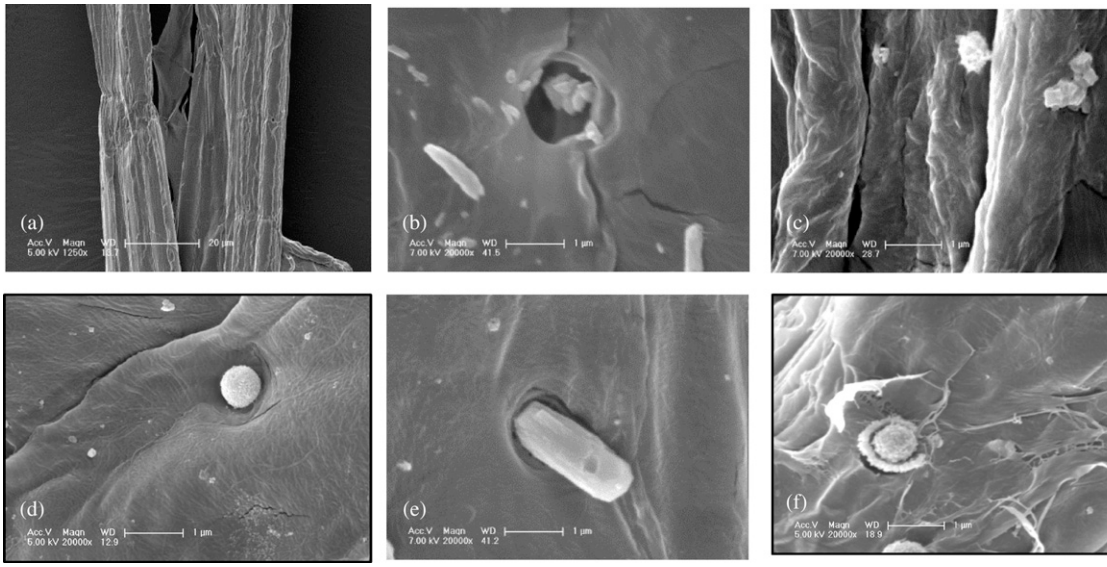

Figure 5. Scanning electron microscopy images of treated bamboo fibers. (a) untreated; (b) 5°C; (c) 15°C; (d) 25°C; (e) 45°C; (f) 65°C.

Table 2. Surface roughness and contact angles of single bamboo fibers.[a]

Treated conditions (°C)	Rq (nm)			Contact angle (°)		
	Mean	SD	LSD	Mean	SD	LSD
Untreated	340.25	133.21	A	65.75	1.78	A
5	175.78	63.53	B	68.07	2.09	B
15	175.46	85.71	B	69.63	1.58	C
25	150.21	62.31	B	70.91	1.37	CD
45	186.75	80.92	B	68.91	2.86	BC
65	294.50	133.58	A	69.57	2.31	CD

[a] SD, standard deviation; LSD, least significant difference. Groups with the same letters indicate that there is no statistical difference ($p < 0.05$) between the samples according to LSD test.

insignificant ($\alpha = 0.05$) during 5-45°C. The lowest surface roughness stood for $CaCO_3$ particles with a suitable size filling the micropores and longitudinal wrinkles of the bamboo fibers and were uniformly distributed across the surface of the fibers, in accordance with well-distributed Ca elementals observed in Fig 4d.

Contact Angle Analysis

Figure 6 shows that as the treated temperature increased, CA increased initially and then decreased slightly. As shown in Table 2, CA of the bamboo fibers increased significantly after the treatments and the mean values of treated fibers reached their maximum at 25°C. The coating of $CaCO_3$ particles may have resulted in a smoother surface and, consequently, a higher Ca content was observed (Chen et al 2011a, 2011b). As the particle sizes grew larger, combined with decreased $CaCO_3$ loading percentages, particles could not be well distributed on the fibers. Therefore, the surfaces became rough again, resulting in a decrease in mean values of CA. These might influence interlacements of fibers and interfacial adhesion between fibers and polymer matrix.

Tensile Properties of Individual Fibers

Tensile property comparison for treated and untreated individual fibers is shown in Table 3.

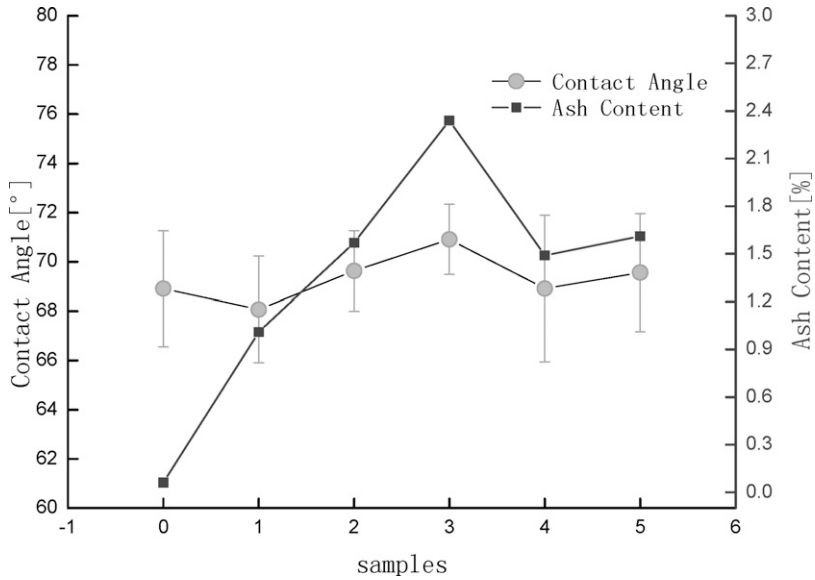

Figure 6. Contact angles of single bamboo fibers. Number 0-5 represents the untreated fibers. Fibers treated at 5, 15, 25, 45, and 65°C, respectively.

Table 3. Tensile properties of individual fibers.

Treated conditions (°C)	Strength (MPa)	Modulus (GPa)	Elongation at break (%)
Untreated	1035.87 (280.37)	27.36 (6.88)	4.21 (1.42)
5	1136.64 (286.82)	29.80 (6.90)	4.09 (0.95)
15	1237.71 (406.61)*	30.70 (8.55)	4.33 (0.90)
25	1383.99 (413.50)**	36.30 (8.92)**	3.89 (0.52)
45	1176.71 (261.80)	31.50 (6.71)*	3.97 (0.66)
65	1167.18 (265.89)	29.43 (8.00)	4.34 (0.91)

Standard deviations are in parentheses. *indicates that there are significant differences at 0.05 level least significant difference (LSD) test. **indicates that there are significant differences at 0.01 level LSD test.

The inorganic nanoparticle treatments improved the tensile properties of the bamboo fibers. Although the elongation at break was not statistically different ($\alpha = 0.05$), the tensile strength and modulus of the fibers increased significantly at $\alpha = 0.01$ after the treatments. Table 3 and Fig 7 indicate that as $CaCO_3$ content increased, tensile strength and modulus increased, elongation at break decreased, and tensile strength and modulus exhibited maximum value at 25°C. A 33.61% increase in tensile strength (from 1.04 to 1.38 GPa) and a 32.39% increase in tensile modulus (from 27.36 to 36.30 GPa) were obtained for the fiber treated at 25°C. The improvement in the tensile modulus should be attributed to the impregnation of $CaCO_3$ particles in fiber cell walls, which increased the density of the fibers and minimized the defects in the fibers by filling up micropores. The $CaCO_3$ particles in fibers also helped to transfer stresses between the cellulose fibrils, improving the overall tensile strength.

Tensile Properties of Treated Bamboo Fiber–Polypropylene Composites

Tensile strength and tensile modulus of treated fiber–PP composites are shown in Table 4. For most treatment conditions, PP composites reinforced with treated fibers showed improvement in both tensile strength and tensile modulus.

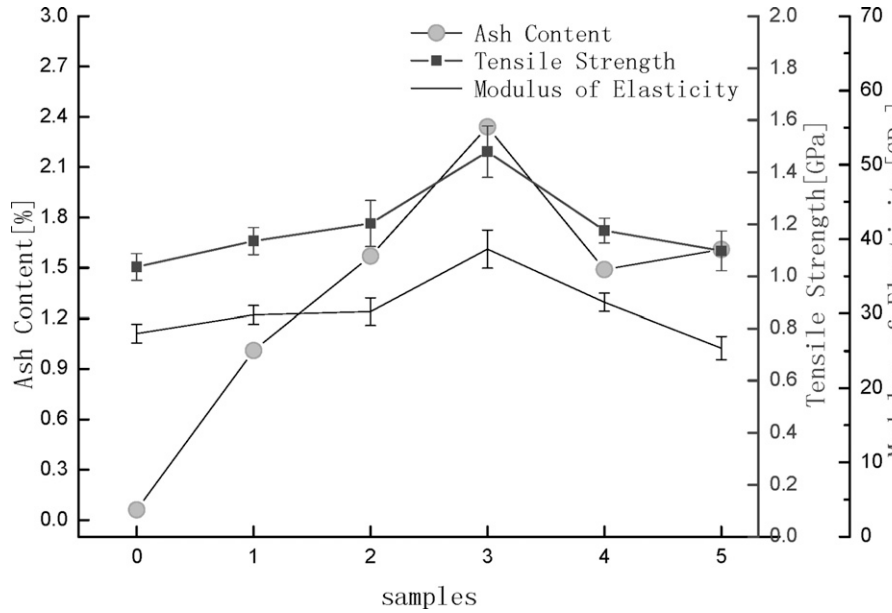

Figure 7. Tensile properties of single bamboo fibers. Number 0-5 represents the untreated fibers. Fibers treated at 5, 15, 25, 45, 65°C, respectively.

Table 4. Tensile strength and modulus of treated bamboo fiber–polypropylene composites.[a]

	Strength (MPa)			Modulus (GPa)		
Treated conditions (°C)	Mean	SD	LSD	Mean	SD	LSD
Untreated	48.91	6.32	A	1.78	0.27	A
5	51.27	7.37	A	1.90	0.27	AB
15	54.49	5.21	BC	1.96	0.22	BC
25	56.04	4.79	C	2.13	0.14	C
45	50.73	5.20	AB	1.86	0.20	AB
65	52.27	5.95	AB	1.88	0.28	AB

[a] SD, standard deviation. Groups with the same letters indicate that there is no statistical difference ($p < 0.05$) between the samples according to least significant difference (LSD) test.

A 14.58% increase in tensile strength and 19.66% increase in tensile modulus were obtained at 25°C, which was the most reinforcing compared with other temperatures. No significant differences in tensile strength and modulus were found in partial treatment conditions.

Mechanical property improvement for the bamboo fiber–PP composites should be attributed to the improvement in interfacial bonding between the treated fibers and the PP matrix. Figure 8 shows scanning electron microscope (SEM) images for the fracture surfaces of fiber–PP composites with both treated and untreated fibers. When composites were broken under a tensile force, some fibers would be pulled out from the fracture surfaces if the fibers and PP matrix were not well bonded. A large amount of fibers were pulled out on the fracture surfaces in the composites with untreated fibers (Fig 8a). This indicated that the interfacial compatibility between untreated fibers and PP matrix was poor. The interfacial compatibility between the treated fibers and the PP matrix was much improved compared with the control samples, indicating stronger adhesion between the fibers and the PP matrix.

Table 4 presents the tensile strength and modulus of the composites made from treated and untreated bamboo fibers. With an increase in temperature up to 25°C, the mechanical property

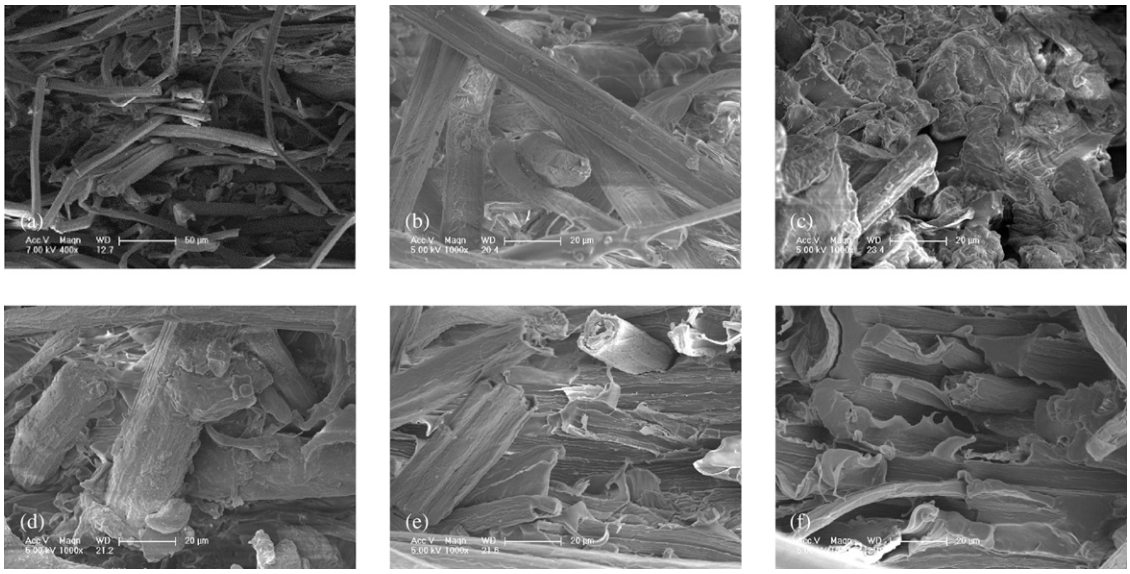

Figure 8. Scanning electron microscopy images of the fracture surfaces of bamboo fiber–polypropylene (PP) composites. (a) untreated; (b) 5°C; (c) 15°C; (d) 25°C; (e) 45°C; (f) 65°C.

of the composites increased gradually. The increase in strength could be attributed to the homogeneously dispersed $CaCO_3$ particles because the well-dispersed particles made the crack propagation path longer, absorbed a portion of the energy, and enhanced composite deformation (Leong et al 2004). It may be reasoned that the inorganic nanoparticles deposited on the fiber surface served as nucleation sites to initiate crystalline formation of the semicrystalline polymer matrix around the fibers.

CONCLUSIONS

Inorganic particles ($CaCO_3$) were successfully impregnated into bamboo fibers with varying treatment temperatures. From the analysis of SEM images and ash analysis, the particle deposition is clearly certified on fiber surfaces. The AFM and CA results demonstrated that the surface of treated individual fibers became smoother with increasing temperature and reached the smoothest at 25°C. The tensile strength of a single fiber was increased by 33.61%, and the tensile modulus was increased by 32.39% through $CaCO_3$ particle treatment in situ. The impregnated inorganic particles improved the compatibility between the fibers and the PP matrix, increasing tensile modulus and tensile strength of the bamboo fiber–PP composites. Tensile strength and modulus for composites made from treated bamboo fibers were increased by 14.58 and 19.66%, respectively.

ACKNOWLEDGMENTS

This research was financed by the China Nature Science Foundation (CNSF) (Award Number 31170525) and National Science Foundation (NSF) CMMI 1247008.

REFERENCES

Alexandre M, Dubois P (2000) Polymer-layered silicate nanocomposites: Preparation, properties and uses of a new class of materials. Mater Sci Eng Rep 28(1-2):1-63.

Allan GG, Negri AR, Ritzenthaler P (1992) The microporosity of pulp: The properties of paper made from pulp fibers internally filled with calcium carbonate. Tappi J 75(3):239-244.

Altay E, Shahwan T, Tanoğlu M (2007) Morphosynthesis of $CaCO_3$ at different reaction temperatures and the effects of PDDA, CTAB, and EDTA on the particle morphology and polymorph stability. Powder Technol 178(3):194-202.

Amaral M, Lopes MA, Santos JD, Silva RF (2002) Wettability and surface charge of Si_3N_4-bioglass composites in contact with simulated physiological liquids. Biomaterials 23(20):4123-4129.

Biswas M, Ray SS (2001) Recent progress in synthesis and evaluation of polymer-montmorillonite nanocomposites. New polymerization techniques and synthetic methodologies, advances in polymer science, Volume 155. Springer, Berlin, pp. 167-221.

Chen H, Wang G, Cheng H (2011a) Properties of single bamboo fibers isolated by different chemical methods. Wood Fiber Sci 43(2):111-120.

Chen H, Wang G, Cheng H, Cao S, Gao J (2011b) Effects of different chemical maceration methods on the surface wetting properties and section shapes of single bamboo fibers. Journal of Beijing Forestry University 33(01):115-118.

Chen J, Yan N (2012) Hydrophobization of bleached softwood kraft fibers via adsorption of organo-nanoclay. Bioresources 7(3):4132-4149.

Chen J, Yan N (2013) Mechanical properties and dimensional stability of organo-nanoclay modified biofiber polymer composites. Compos, Part B Eng 47:248-254.

Cheng H, Wang G, Shen X, Chen H, Zhang S (2013) Single fiber contact angle measured by different methods and correlation analysis. China Forest Products Industry 40:49-51.

Deka BK, Maji TK (2011) Study on the properties of nanocomposite based on high density polyethylene, polypropylene, polyvinyl chloride and wood. Compos Part A-Appl S 42(6):686-693.

GB (2006) T 1040.3-2006. Plastics. Determination of tensile properties. Part 3: Test conditions for films and sheets. Standardization Administration of the People's Republic of China, Beijing, China.

GB (2009) T 742-2008. Fibrous raw material, pulp, paper and board—Determination of ash. Standardization Administration of the People's Republic of China, Beijing, China.

Gopi SP, Subramanian VK (2012) Polymorphism in $CaCO_3$—Effect of temperature under the influence of EDTA (di sodium salt). Desalination 297:38-47.

Green HVDD (1985) Lumen-loaded paper pulp, its production and use. US Patent 4,510,020.

Huang JH, Mao ZF, Luo MF (2007) Effect of anionic surfactant on vaterite $CaCO_3$. Mater Res Bull 42(12):2184-2191.

Jacob A (2006) WPC industry focuses on performance and cost. Reinforced Plastics 50(5):32-33.

Khunová V, Hurst J, Janigová I, Smatko V (1999) Plasma treatment of particulate polymer composites for analyses by scanning electron microscopy: II. A study of highly filled polypropylene/calcium carbonate composites. Polym Test 18(7):501-509.

Kuusipalo J, Kaunisto M, Laine A, Kellomaki M (2005) Chitosan as a coating additive in paper and paperboard. Tappi J 4(8):17-21.

Leong YW, Ishak ZAM, Ariffin A (2004) Mechanical and thermal properties of talc and calcium carbonate filled polypropylene hybrid composites. J Appl Polym Sci 91(5):3327-3336.

Lutton CW (1952) Production of pigmented cellulosic pulp. US Patent 2,583,548.

Mannelquist A, Almqvist N, Fredriksson S (1998) Influence of tip geometry on fractal analysis of atomic force microscopy images. Appl Phys A-Mater 66(1):S891-S895.

Raj RG, Kokta BV, Grouleau G, Daneault C (1990) The influence of coupling agents on mechanical properties of composites containing cellulosic fillers. Polymer-Plastics Technology and Engineering 29(4):339-353.

Schmidt D, Shah D, Giannelis EP (2002) New advances in polymer/layered silicate nanocomposites. Curr Opin Solid St M 6(3):205-212.

Shi J, Shi S, Barnes HM, Horstemeyer MF, Wang G (2011) Kenaf bast fibers — Part II: Inorganic Nanoparticle Impregnation for Polymer Composites. International Journal of Polymer Science. Volume 2011, Article ID 736474, 7 pages (doi:10.1155/2011/736474).

Tang W, Wang Y (2012) Fractal characterization of impact fracture surface of steel. Appl Surf Sci 258(10):4777-4781.

Wan J, Wang Y, Xiao Q (2010) Effects of hemicellulose removal on cellulose fiber structure and recycling characteristics of eucalyptus pulp. Biores Technol 101(12):4577-4583.

Wang G, Yu Y, Shi S, Wang J, Cao S, Cheng H (2011) Microtension test method for measuring tensile properties of individual cellulosic fibers. Wood Fiber Sci 43(3):251-261.

Wu XF, Dzenis YA (2006) Droplet on a fiber: Geometrical shape and contact angle. Acta Mech 185(3-4):215-225.

Yamaki J, Katayama Y (1975) New method of determining contact angle between monofilament and liquid. J Appl Polym Sci 19(10):2897-2909.